

# Multichannel Seismic Survey of Lake Azuei (Haiti) Documents a Complex System of Active Transpressional Structures Across the North American-Caribbean Plate Boundary

Marie-Helene Cormier<sup>1</sup>, Nestor Charles<sup>2</sup>, Heather Sloan<sup>3</sup>, Nigel Wattrus<sup>4</sup>, Christopher Sorlien<sup>5</sup>, Dominique Boisson<sup>2</sup>, Kelly Guerrier<sup>2</sup>, Casey Hearn<sup>6</sup>, John King<sup>6</sup>, Roberte Momplaisir<sup>2</sup>, Steeve Symithe<sup>2</sup>, and Sophia Ulysse<sup>2</sup>

<sup>1</sup>U. Rhode Island, Graduate School of Oceanography, Narragansett, RI, USA

<sup>2</sup>Université d'Etat d'Haïti, URGeo, Port-au-Prince, Haiti

<sup>3</sup>City Univ. New York - Lehman College, Bronx, NY, USA

<sup>4</sup>Univ. Minnesota, Duluth, MN, USA

<sup>5</sup>Univ. California Santa Barbara, CA, USA

<sup>6</sup>Univ. Rhode Island, GSO, Narragansett, RI, USA

November 22, 2022

## Abstract

To a first order, the Caribbean plate converges obliquely at  $\sim 2$  cm/yr toward the North American plate. This transpression is partly accommodated across the island of Hispaniola by the partitioning of motion between a fold-and-thrust belt trending NW-SE, and two E-W left-lateral fault systems located 150 km apart. The southern fault, the Enriquillo-Plantain Garden Fault (EPGF), is morphologically well expressed in western Haiti but its precise geometry in eastern Haiti is debatable. There, Lake Azuei stretches over 20 km in a direction parallel to the fold-and-thrust belt while its southern shoreline strikes EW, parallel to the expected trend of the EPGF. Because of a high sedimentation rate, the history of transpressional deformation should be captured in the lake stratigraphy and, accordingly, we acquired 220 km of multichannel seismic reflection (MCS) profiles across its surface. The survey followed a grid pattern with a spacing of 1.2 km and achieved a penetration of up to 300 m beneath lakebed. Interpretation of the dataset documents two major structures. First, the western side of the lake is occupied by a broad NW-trending monoclinical fold. This fold is cross-cut by a few NW-striking vertical (strike-slip) faults. We propose that this monocline is the surface expression of a SW-dipping blind thrust fault. The progressive steepening of the seismic horizons with depth suggests that it has been continuously active during the deposition of at least 300 m of sediments. The other major structure consists of a  $\sim 2$  km-wide deformation zone that borders the EW-trending southern shore. This deformation zone is faintly imaged below a shallow gas front. We tentatively propose that it corresponds to a set of fault-propagation folds that are developing ahead of an EW, S-dipping oblique-slip fault. Such a model has been proposed already from three other independent studies involving GPS monitoring, seismological monitoring, and detailed field mapping. It is also supported by CHIRP profiles acquired concurrently with our MCS data and that document folding of the topmost turbidites but a lack of evidence for any stratigraphic offset across faults. Furthermore, a set of en echelon folds in that area are trending EW, while WNW-ESE fold axes would be expected instead above an EW vertical strike-slip fault.

## Summary

The Caribbean plate converges obliquely at ~2 cm/yr toward the North American plate (Figure 1). This transpression is partly accommodated across the island of Hispaniola by the partitioning of motion between a fold-and-thrust belt trending NW-SE, and two E-W left-lateral fault systems. The southern fault, the Enriquillo-Plantain Garden Fault (EPGF), is morphologically well expressed in western Haiti but its precise geometry in eastern Haiti is debatable. There, Lake Azuei stretches over 20 km in a direction parallel to the fold-and-thrust belt while its southern shoreline strikes EW, parallel to the expected trend of the EPGF. We acquired 220 km of multichannel seismic reflection (MCS) profiles across its surface. This dataset documents the following structures:

- 1) The western side of the lake is occupied by a broad NW-trending monoclinical fold (Figures 2 & 3). We propose that this monocline is the surface expression of a SW-dipping, NW-striking blind thrust fault. The progressive steepening of the seismic horizons with depth (Figures 2, 3, and 5) suggests that it has been continuously active during the deposition of at least 300 m of sediments.
- 2) A ~2 km-wide deformation zone borders the EW-trending southern shore (see map poster T31D-0268, at left). This deformation zone is faintly imaged below a shallow gas front (Figure 4). We propose that it corresponds to a series of fault-propagation folds that develop ahead of an EW, S-dipping oblique-slip fault. This interpretation is compatible CHIRP profiles acquired concurrently with our MCS data and that document folding of the topmost turbidites but a lack of evidence for any stratigraphic offset across faults (see poster T31D-0268, at left).
- 3) A NW-trending fold imaged between the monoclinical fold to the west and the Matheux Mountain to the east indicates that on-going tectonic deformation affects the entire length and width of the lake (Figure 6).

## Two tectonic models

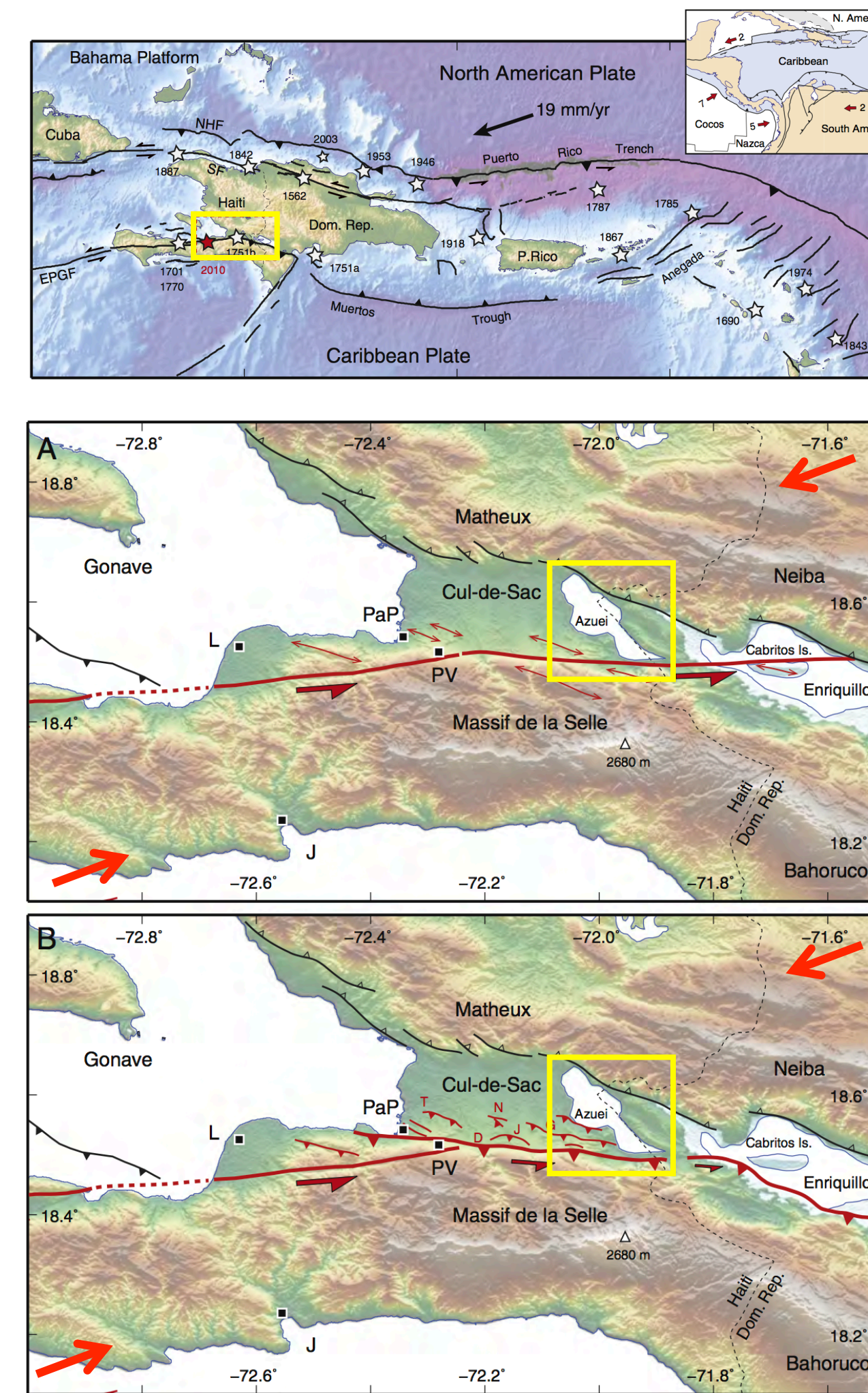


**Figure 1.** Tectonic context (after Symithe & Calais, 2016). Two models have been proposed for the eastern termination of the EPGF near Lake Azuei.

**Top model:** The EPGF is a continuous, vertical, strike-slip fault associated with minor en échelon drag folds (Mann et al., 1995) and possibly a N-dipping reverse fault subparallel to its strike (Wang et al., 2018)

**Bottom model:** The EPGF transitions eastward into an oblique-slip fault that dips southward beneath the Massif de la Selle (Saint Fleur et al., 2015 & 2019; Symithe & Calais, 2016; Possee et al., 2019)



A 10 m-long boat was trucked to the lake for the seismic survey.

## Results

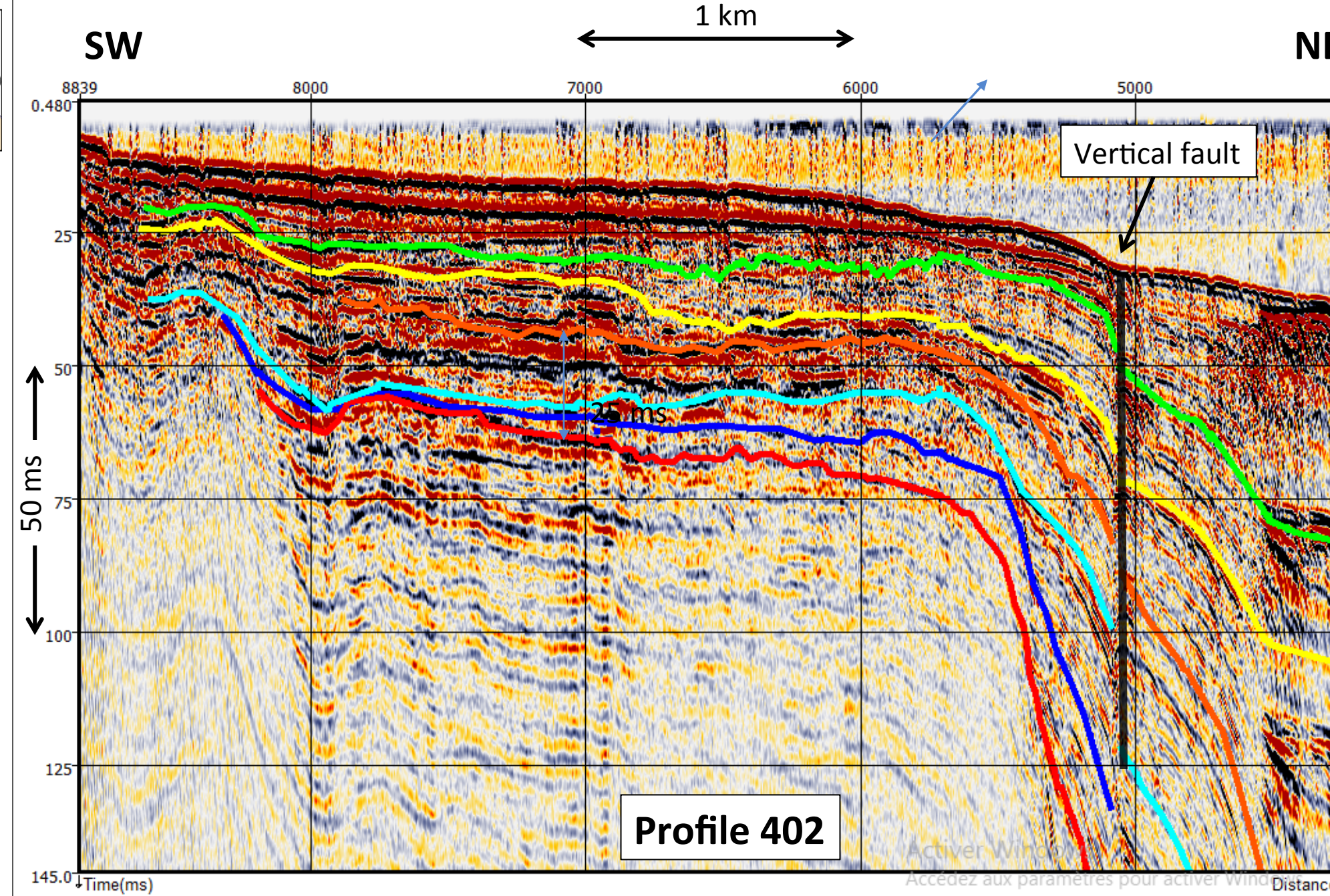


**Figure 2.** A monoclinical fold in the western part of the lake extends ~12 km in a northwesterly direction. The dip of seismic horizons increases with depth, indicate continuous deformation for at least the time necessary to deposit about 300 m of sediments. We propose that this monocline is the surface expression of SW-dipping, NW-striking blind thrust fault. A vertical (strike-slip?) fault locally offsets the monocline.

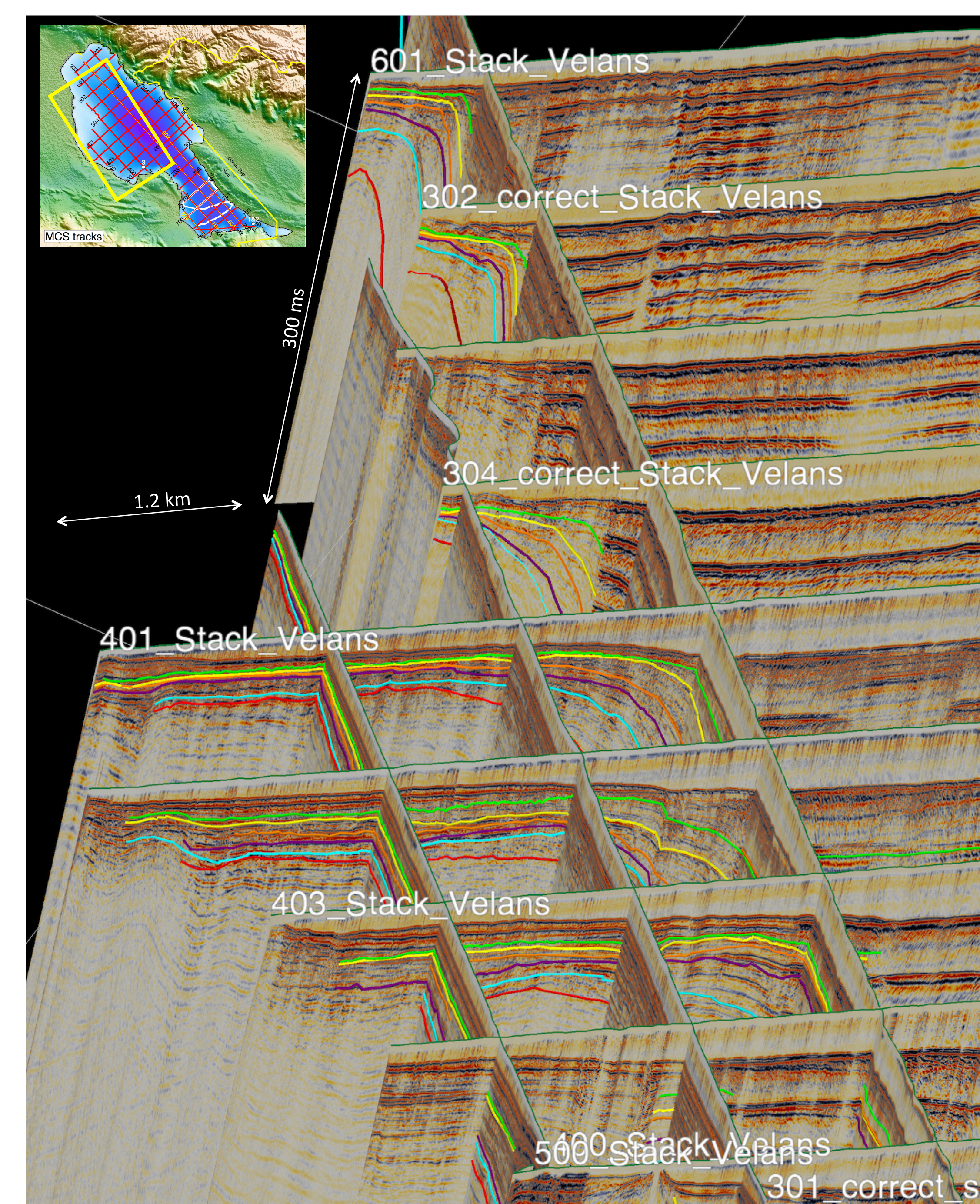


**Figure 3.** MCS profiles image a large monoclinical fold on the west side of Lake Azuei. A shallow gas front is absent in that area of the lake and seismic horizons can be tied from profile to profile.

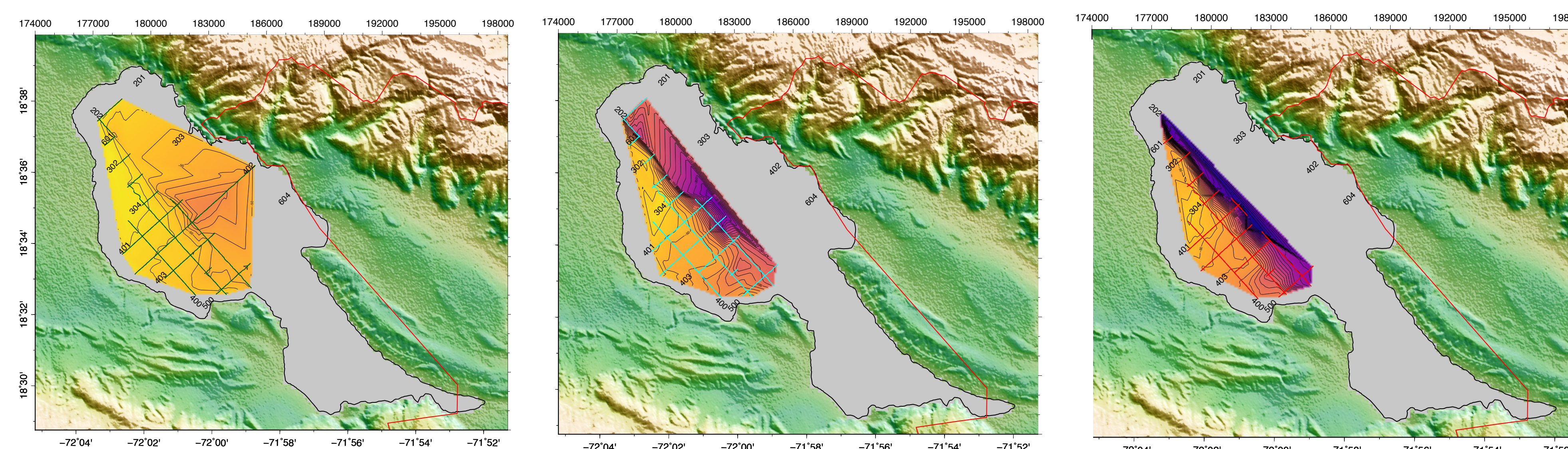


**Figure 5.** Horizon surfaces (in ms) highlight the progressive steepening of seismic horizons beneath the monoclinical fold. Colored lines indicate where identifications of the respective horizons were possible, and the surfaces are extrapolated from these. From left to right, maps correspond to the green horizon (shallower), cyan horizon (intermediate) and red horizon (deeper).

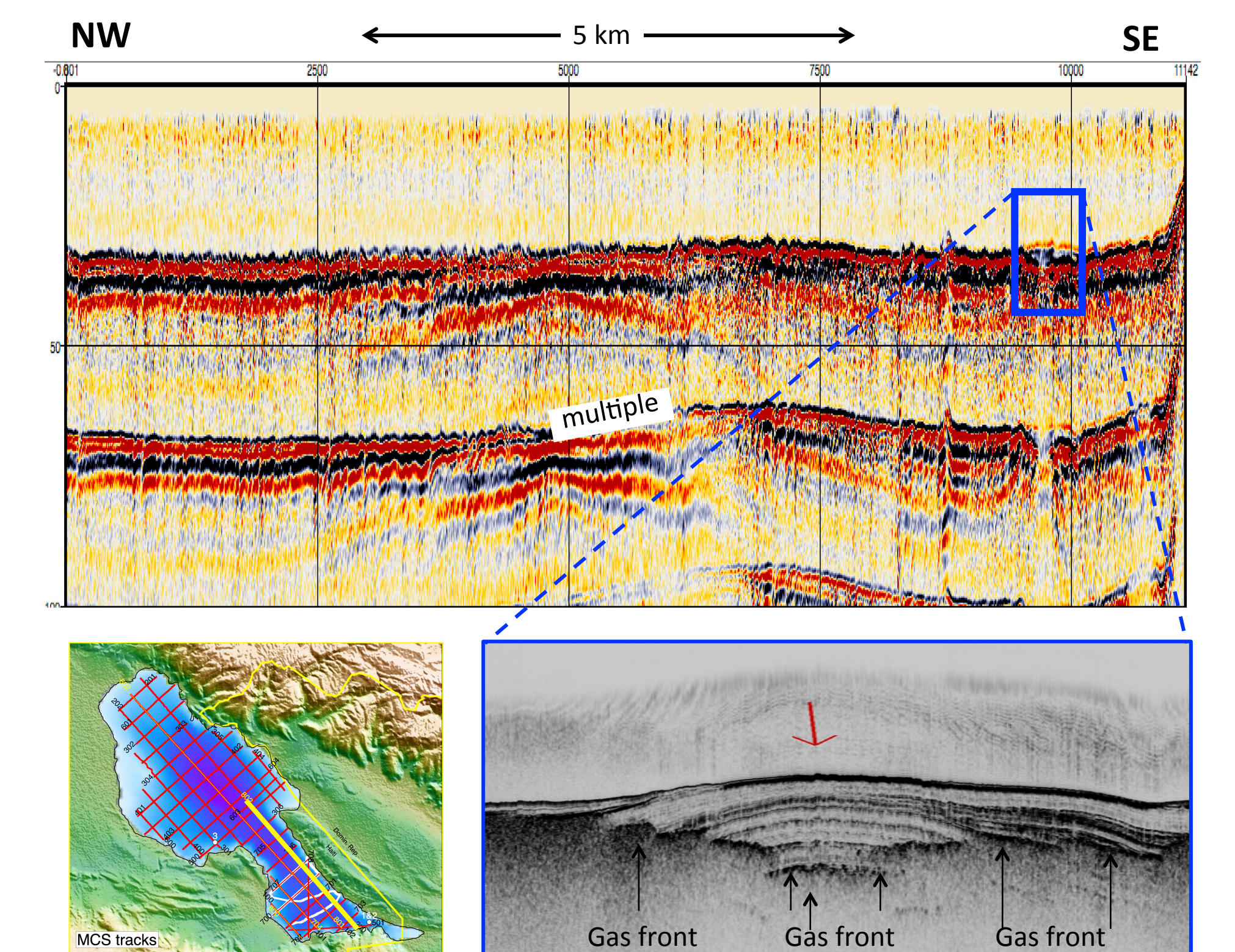


**Figure 4.** Seismic line 802 crosses the SE part of the lake. A deformation zone is faintly visible on the MCS profile (top) beneath a shallow gas front detected on the corresponding CHIRP profile (bottom). Because of the attenuation of the seismic amplitude beneath the gas front, it remains unclear whether this deformation zone reflects faulting and/or folding. However, given the presence of well-imaged EW-trending shallow folds in CHIRP profiles, we favor a model where it reflects fault propagation folding ahead of a S-dipping oblique-slip fault (second model at left).

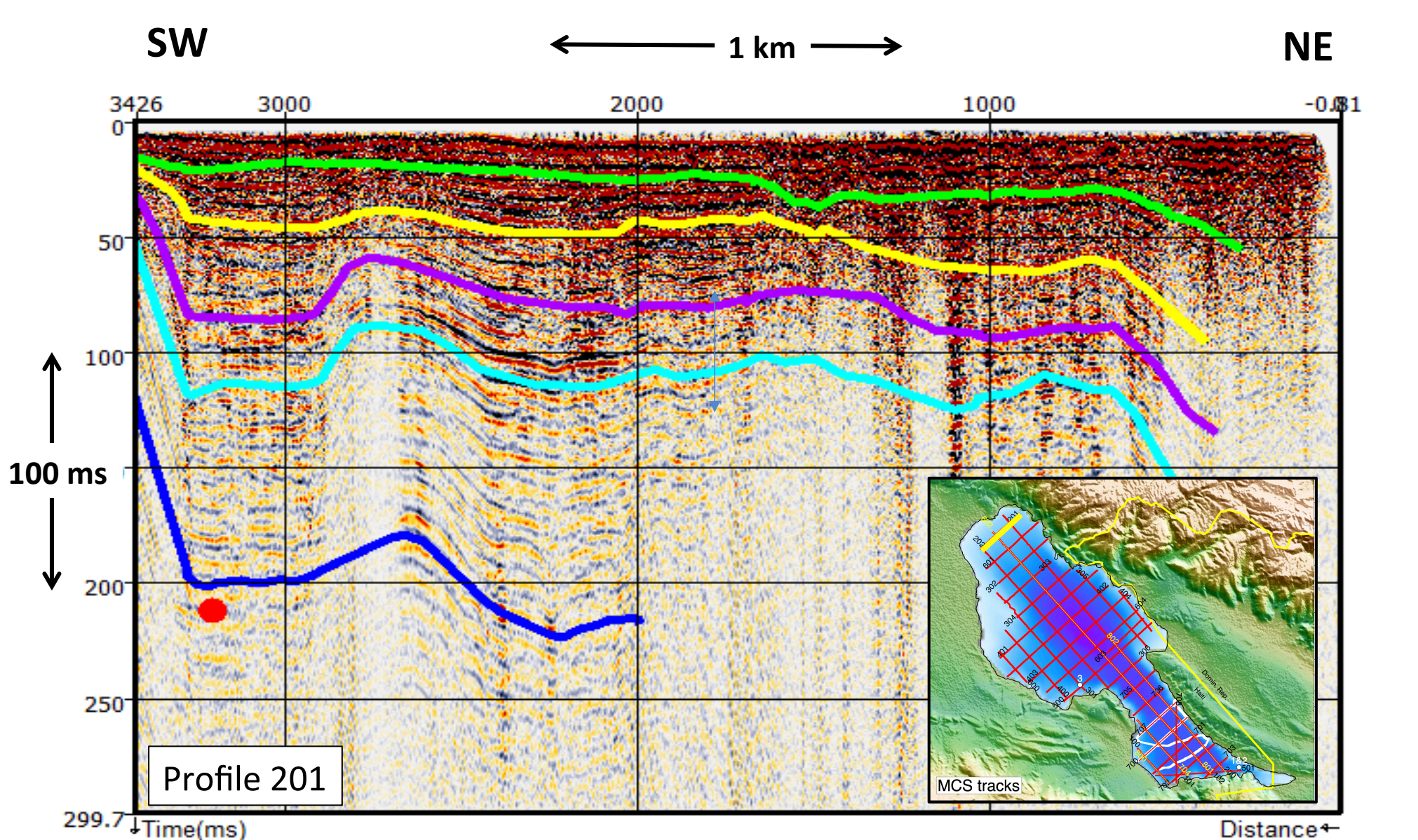
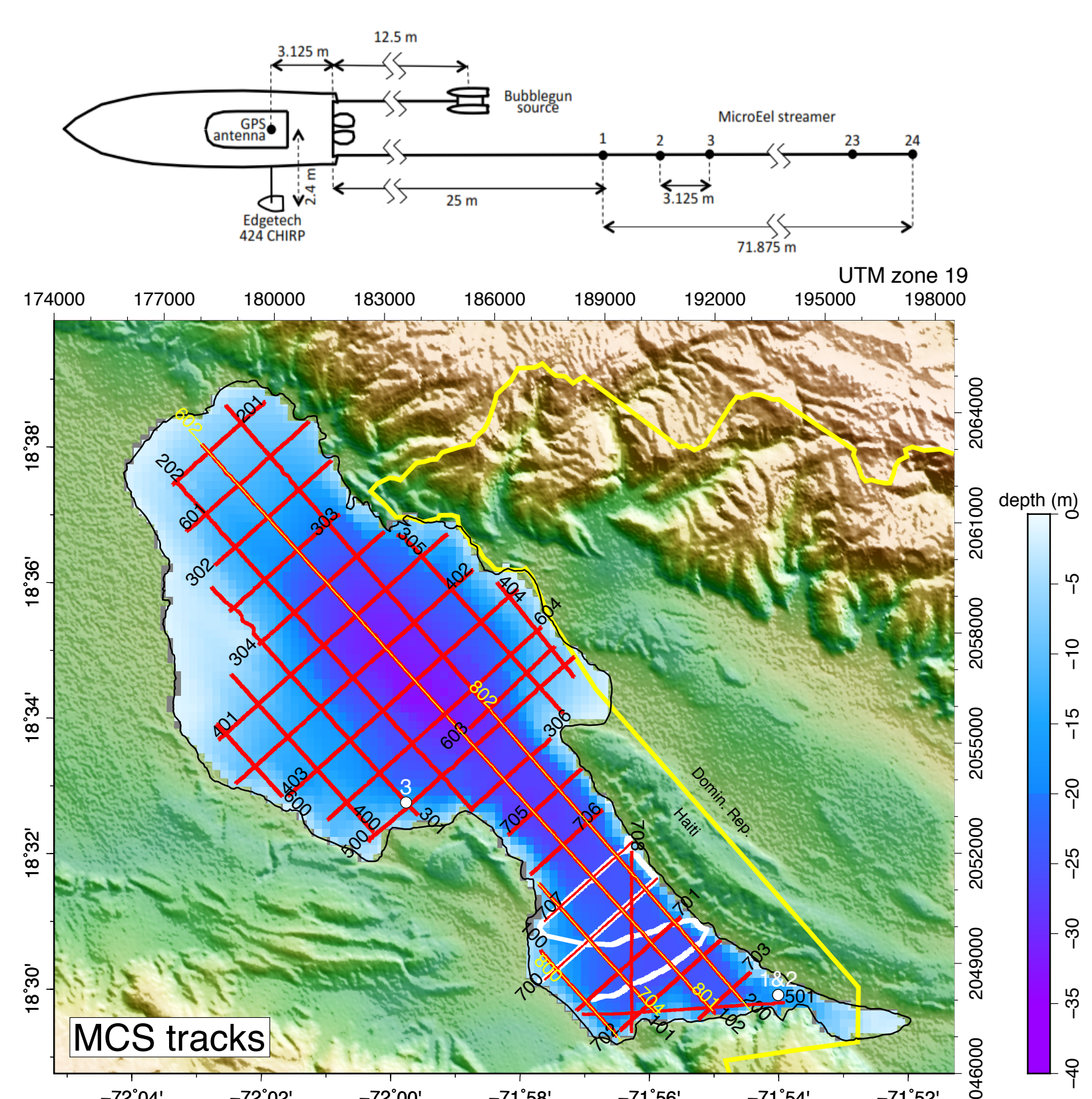


**Figure 6.** MCS profiles reveal the presence of a fold about ~1 km-wide in the northern part of the lake. That fold trends NW, parallel to the monoclinical fold as well as the Matheux mountains; it is also detected in the bathymetry (see poster T31D-0268 at left). Its presence indicates on-going tectonic deformation also affects the north end of the lake.

## Data and Methods

MCS profiles were acquired on a regular grid with a 1.2 km track spacing, using a 24 channels, 75 m-long streamer. CMP gathers are 24-fold and maximum record length is 300 ms. Processing to-date includes velocity analysis and stacking.



## References

Mann et al., Tectonophysics, 246, 1-69, 1995.  
 Possee et al., Tectonics, 38, 1138-1155, 2019.  
 Saint Fleur et al., Geophys. Res. Lett., 42, 10273-10281, 2015 / Saint Fleur et al., Tectonophysics, 771, 228235, 2019.  
 Symithe & Calais, Tectonophysics, 679, 117-124, 2016.  
 Wang et al., Tectonics 37, 3834-3852, doi: 10.1029/2017TC004920, 2018.